European Journal of Radiology 120 (2019) 108695

Contents lists available at ScienceDirect

European Journal of Radiology

journal homepage: www.elsevier.com/locate/ejrad

Research article

Whole-body diffusion-weighted MRI for evaluation of response in multiple myeloma patients following bortezomib-based therapy: A large single-center cohort study

Yu Zhang[a], Xing Xiong[a], Zhengzheng Fu[b], Hui Dai[a], Feirong Yao[a], Dong Liu[a], Shengming Deng[c,*], Chunhong Hu[a,*]

[a] Department of Radiology, The First Affiliated Hospital of Soochow University, Suzhou, 215006, Jiangsu, China
[b] Department of Hematology, The First Affiliated Hospital of Soochow University, Suzhou, 215006, Jiangsu, China
[c] Department of Nuclear Medicine, The First Affiliated Hospital of Soochow University, Suzhou, 215006, Jiangsu, China

ARTICLE INFO

Keywords:
Multiple myeloma
Whole-body diffusion-weighted MRI
Bortezomib

ABSTRACT

Purpose: To determine the feasibility of whole-body diffusion-weighted imaging (WB-DWI) MRI for evaluation of response in patients with multiple myeloma (MM) following bortezomib-based therapy and to explore the direction of apparent diffusion coefficient (ADC) changes upon treatment.

Method: Seventy-two MM patients who underwent WB-DWI MRI before and after bortezomib-based chemotherapy (21 weeks) were evaluated retrospectively. The estimated tumor volume (eTV) and ADC_{mean} values before and after chemotherapy were calculated and compared between deep and non-deep responders. Predictive value of baseline ADC_{mean} was calculated to predict the trend of ADC_{mean} change following treatment.

Results: Fifty-five patients were classified as deep responders, and 17 cases were assigned as non-deep responders. For 327 focal lesions (FLs), the ADC_{mean} value was significantly increased from baseline to post-treatment. However, the ADC_{mean} value was significantly decreased following treatment in 846 representative diffuse lesions. Diffuse lesions showed a significantly decreased ADC_{mean} value in deep responders, whereas no significant variation in ADC_{mean} value in FLs was found between deep and non-deep responders. Baseline ADC_{mean} at a specific value (0.808×10^{-3} mm^2/s) yielded a maximum specificity (68.05%) and sensitivity (54.09%) in predicting increase of post-treatment ADC_{mean}.

Conclusions: The ADC_{mean} value was significantly decreased in MM patients with diffuse pattern, while it was significantly increased in those with focal pattern following bortezomib-based treatment. WB-DWI MRI could be used to discriminate deep response to induction treatment in MM patients with diffuse infiltration pattern. Baseline ADC_{mean} value might have a potential to predict the trend of ADC_{mean} change following treatment.

1. Introduction

As a clonal hematologic malignancy, multiple myeloma (MM) is characterized by the accumulation of monoclonal plasma cells in the bone marrow of the axial and appendicular skeletons [1,2]. MM is considered an incurable hematologic malignancy but also a highly treatable disease [3]. With the introduction of novel agents, such as bortezomib (a first-generation PI), the prognosis of MM patients has been significantly improved [4]. Despite the advancements in the treatment, intrinsic or acquired therapy resistance as well as tumor relapse or recurrence are still commonly observed in clinical practice. Therefore, an accurate evaluation of response to treatment is very important to secure effective therapy.

Traditionally, therapeutic response in MM is assessed through the

Abbreviations: ^{18}F-FDG PET/CT, ^{18}F-fluorodeoxyglucose positron emission tomography/computed tomography; ADC, Apparent diffusion coefficient; ANOVA, One-way analysis of variance; AUC, Area under the curve; CR, Complete response; eTV, Estimated tumor volume; FA, Flip angle; FLs, Focal lesions; IMWG, International Myeloma Working Group; MM, Multiple myeloma; MR, Minimal response; NSA, Number of signals acquired; PD, Progressive disease; PR, Partial response; ROC, Receiver operating characteristics; ROIs, Regions of interest; sCR, Stringent complete remission; SD, Stable disease; TE, Echo time; TI, Inversion time; TIM, Total imaging matrix; TIRM, T2 turbo inversion recovery magnitude; TR, Repetition time; VGPR, Very good partial response; WB-DWI, Whole-body diffusion-weighted imaging

* Corresponding authors.
E-mail addresses: dshming@163.com (S. Deng), sudahuchunhong@163.com (C. Hu).

https://doi.org/10.1016/j.ejrad.2019.108695
Received 18 April 2019; Received in revised form 14 August 2019; Accepted 26 September 2019

International Myeloma Working Group (IMWG) criteria based on indirect measurements of biological markers, including serum and urine monoclonal protein concentrations, serum free light chain ratio and proportion of clonal plasma cells in bone marrow [5]. However, M-protein is a surrogate marker, which may be missing or unreliable (e.g. nonsecretory or extramedullary MM). On the other hand, these bone marrow-based techniques have limitations due to invasion and random sampling [6]. In the past decade, modern imaging techniques, such as whole-body magnetic resonance imaging (WB-MRI) and ^{18}F-fluorodeoxyglucose positron emission tomography/computed tomography (^{18}F-FDG PET/CT), play a growing role in diagnostics, therapy monitoring and follow-up of MM patients.

Diffusion-weighted imaging (DWI) is a functional MRI, which determines the random movement of water molecules within tissues. It is firstly established in the neuroradiology for the detection of brain ischemia, and it has been subsequently extended to oncological applications [7]. DWI-MRI is highly sensitive for the detection of bone marrow infiltration in newly diagnosed MM patients [8] Based on existing and emerging evidence, the IMWG recommends WB-MRI as the imaging modality of choice for pretreatment assessment of MM [9].

Recently, several studies have demonstrated that apparent diffusion coefficient (ADC) value derived from DWI-MRI can be used as a valuable parameter for evaluating the treatment response of MM patients. However, there is a controversy on the change of ADC value following treatment. Most data have demonstrated that ADC value derived from WB-DWI MRI is significantly increased in the lesions of patients who respond to treatment [10–13], while other studies have reported that ADC value is decreased in MM patients responding to treatment [14–16]. Therefore, we aimed to determine the feasibility of WB-DWI MRI for evaluation of response in MM patients following bortezomib-based therapy and to explore the direction of ADC changes upon treatment.

2. Materials and methods

This retrospective study was approved by the Ethics Committee of the First Affiliated Hospital of Soochow University, with waiver of informed consent.

2.1. Patients

Patients with histologically and laboratory proven MM between April 2015 and January 2019 were enrolled in this analysis. WB-DWI MRI was performed at the time of diagnosis (baseline) and the end of induction treatment (four to five cycles of bortezomib-based chemotherapy). The following patients were excluded from our study: 1) patients with normal bone marrow appearance; 2) MM patients who had additional malignancies; 3) time interval between baseline and post-treatment scans < 14 weeks or > 25 weeks; 4) patients who received radiation therapy; and 5) patients who received granulocyte colony-stimulating factor. Treatment response was evaluated according to the IMWG response criteria [6]. In the present study, very good partial response (VGPR), complete response (CR) and stringent complete remission (sCR) were deemed as deep response. Clinical outcomes, including progressive disease (PD), minimal response (MR), partial response (PR) and stable disease (SD), were deemed as non-deep response.

2.2. Image acquisition

All examinations were performed on a 3.0 T MRI scanner (Magnetic Verio, Siemens Healthcare, Erlangen Germany) equipped with a Total imaging matrix (TIM) system. The patients were positioned supine and scanned in the magnet bore with head first. Phased-array surface coils were installed to cover from the head to the upper femur.

Our WB MRI protocol consisted of the following sequences. T2 turbo inversion recovery magnitude (TIRM) sequence [turbo factor, 26; echo time (TE), 84 ms; repetition time (TR), 7110 ms; inversion time (TI), 220 ms; flip angle (FA), 150; number of signals acquired (NSA) 1; number of slices, 31; slice thickness, 5 mm; slice gap, 1.5 mm; FOV, 480 mm; scan time, 6 min; voxel size, 0.9 × 0.9 × 5.0 mm^3] was acquired on the coronal plane from the head to the upper femur. On the same coverage area, axial DWI sequences were acquired using two different b values (b = 50, 700 s/mm^2) with the following parameters: echo planar imaging (EPI); TR 4000 ms; TE, 46 ms; slice thickness, 5 mm; slice gap, 0; FOV, 450 mm; number of slices, 31; scan time, 17 min; voxel size, 1.5 × 1.5 × 5.0 mm^3. All images were acquired during free breathing. The total acquisition time was about 23 min. No contrast medium was given.

At the end of the study, all images were reconstructed using the software integrated in the scanner to generate coronal WB T2 TIRM and DWI. Subsequently, inverted-gray-scale and pseudocolor processing "PET-like" images were obtained for radiologists at the time of evaluation.

2.3. WB-MRI quantitative analysis

Images were reviewed by two independent radiologists with more than 10 years of experience who had no access to patient characteristics, laboratory findings, type of therapy and the results of all other imaging. Differences in evaluation between the two radiologists were resolved by consensus.

WB-MRI in MM was interpreted according to the Myeloma Response Assessment and Diagnosis System (MY-RADS) [17].

According to their infiltration pattern of DWI MRI, patients were divided into three groups as follows: focal, diffuse (including salt-and-pepper) and mixed (focal and diffuse) groups [18].

Focal lesions (FLs) were defined as those focal areas with high signal intensity on TIRM, restricted diffusion returning high signal intensity on DWI b_{700} images compared with surrounding marrow, and a diameter of at least 5 mm. In order to conduct a comprehensive and practical analysis of tumor sites in the entire skeleton, a maximum of 20 FLs per patient were selected according to the Durie-Salmon PLUS staging system [13,19]. The regions of compression fracture, the basivertebral vessels and any focal nonmyelomatous lesions, including inflammatory degenerative endplate changes, Schmorl nodes and hemangiomas, were excluded.

For the diffuse pattern, the axial skeleton was divided into 10 anatomical locations (cervical spine, thoracic spine, lumbar spine, pelvis, clavicle, shoulder girdle, humerus, chest wall, femur and lower leg, and sternum). For each anatomical location involved, the ADC_{mean} values of three different tumor sites were measured.

Regions of interest (ROIs) were centrally placed within the hyperintense area of the tumor on DWI with b = 700 s/mm^2 value using a separate workstation (syngo.via, Siemens, Germany). The mean ADC value of the same FL was documented at baseline and at follow-up.

Measurement of estimated tumor volume (eTV) was performed for quantitative image analysis. For patients with no more than five FLs, the largest eTV of every lesion > 1 cm on DWI was measured. When at least five FLs were present, the five largest ones with a diameter of at least 1 cm at pretreatment examination were chosen as target lesions for evaluation of changes in tumor size following therapy. Individual lesion volume was calculated from 3-axis measurements using the caliper tool on b_{700} DWI (Z) images. eTV was calculated as (X × Y × Z/2). A volume of 0 mm^3 was recorded when a lesion disappeared.

2.4. Statistical analysis

Statistical analysis was performed using IBM SPSS 19.0 software (SPSS Inc., Chicago, IL, USA) and GraphPad Prism 5.0 software (GraphPad Software Inc., San Diego, CA, USA). Distribution normality was assessed using a Kolmogorov-Smirnov test. Changes of ADC_{mean}

value between baseline and follow-up were assessed by the two-tailed paired t-test. A two-tailed Wilcoxon matched-pairs signed rank test was used for paired samples that were not normally distributed. The significance of differences between more than two groups was evaluated by one-way analysis of variance (ANOVA). Changes of ADC_{mean} and eTV values between deep responders and non-deep responders were compared. In a subgroup analysis, studies were stratified according to infiltration pattern. For the FL group, differences in ADC_{mean} and eTV values between baseline and follow-up were evaluated. $P < 0.05$ was considered as statistically significant.

For prediction of deep response and ADC increase after treatment, receiver operating characteristics (ROC) curves were derived for percentage change in ADC_{mean} and baseline ADC_{mean}, respectively. The area under the curve (AUC) was quantified to assess performance to discriminate the increase of post-treatment ADC_{mean} across all possible diagnostic thresholds.

3. Results

3.1. Patient characteristics

A total of 83 patients were identified according to our inclusion criteria, while 11 patients were excluded from the present study (five patients with normal bone marrow appearance, and six patients with time interval between baseline and post-treatment scans < 14 weeks or > 25 weeks). Finally, 72 patients, including 43 males and 29 females, (mean age ± SD, 57 ± 9 years; range, 29–74 years) were retrospectively enrolled in the study, with a mean interval of 21 weeks (range 14–25 weeks) between the two examinations. Out of the 72 patients, 55 patients were classified as deep responders (five had sCR, 17 had CR and 33 had VGPR), while the rest were classified as non-deep responders (one with PD, two with SD, two with MR, and 12 with PR). Table 1 lists the detailed characteristics of patients.

Table 1
Characteristics of patients.

Patient characteristics (N = 72)	number or median (range)
Age	57 (29-74)
Sex, male/female:	43:29
Multiple myeloma isotype	
IgG κ	18
IgG λ	17
IgA κ	7
IgA λ	8
IgD λ	7
Light chain	15
Induction regimen	
PAD	45
BTD	17
BD	4
VCD	4
VRD	2
ISS stage	
I	13
II	32
III	27
DSS stage	
I	0
II	4
III	68

Abbreviations: PAD: bortezomib, doxorubicin, dexamethasone; BTD: bortezomib, thalidomide, dexamethasone; BD: bortezomib, dexamethasone; VCD: bortezomib, cyclophosphamide, dexamethasone; VRD: bortezomib, lenalidomide, dexamethasone; ISS: International Staging System; DSS: Durie-Salmon Staging System.

3.2. Per patient analysis

The mean ADC_{mean} value from all measured lesions was determined for each patient at baseline and post-treatment. Fig. 1 presents the per patient analysis for changes of ADC_{mean}. The mean baseline ADC_{mean} of all patients at baseline and post-treatment was $0.80 \pm 0.19 \times 10^{-3}$ mm^2/s and $0.89 \pm 0.55 \times 10^{-3}$ mm^2/s, respectively. There was no significant change in mean ADC_{mean} value following treatment in all patients ($p = 0.11$). Following treatment, there was no significant change of ADC_{mean} in the deep responder group ($0.82 \pm 0.20 \times 10^{-3}$ mm^2/s *vs.* $0.87 \pm 0.58 \times 10^{-3}$ mm^2/s, $p = 0.438$), while a significant increase of ADC_{mean} was observed in the non-deep responder group ($0.74 \pm 0.16 \times 10^{-3}$ mm^2/s *vs.* $0.95 \pm 0.46 \times 10^{-3}$ mm^2/s, $p = 0.036$).

On WB-DWI MRI, infiltration patterns were diffuse in 41/72 (56.94%) patients (including four patients with a “salt-and-pepper” pattern), focal in 12/72 (16.67%) patients, and mixed in 19/72 (26.39%) patients. For patients with diffuse pattern, the ADC_{mean} value was significantly decreased from baseline to post-treatment ($0.73 \pm 0.14 \times 10^{-3}$ mm^2/s *vs.* $0.58 \pm 0.30 \times 10^{-3}$ mm^2/s, $p = 0.004$). Moreover, the ADC_{mean} value was significantly decreased following treatment in deep responders ($0.74 \pm 0.13 \times 10^{-3}$ mm^2/s *vs.* $0.53 \pm 0.23 \times 10^{-3}$ mm^2/s, $p = 0.000$). In the non-deep responder group, the ADC_{mean} remained barely unchanged following treatment ($0.70 \pm 0.15 \times 10^{-3}$ mm^2/s *vs.* $0.74 \pm 0.42 \times 10^{-3}$ mm^2/s, $p = 0.725$).

For patients with focal pattern, the ADC_{mean} value was significantly increased from baseline to post-treatment ($1.02 \pm 0.28 \times 10^{-3}$ mm^2/s *vs.* $1.59 \pm 0.58 \times 10^{-3}$ mm^2/s, $p = 0.005$). Moreover, the ADC_{mean} value was significantly increased following treatment in deep responders ($1.07 \pm 0.30 \times 10^{-3}$ mm^2/s *vs.* $1.62 \pm 0.65 \times 10^{-3}$ mm^2/s, $p = 0.032$) and non-deep responders ($0.89 \pm 0.16 \times 10^{-3}$ mm^2/s *vs.* $1.48 \pm 0.35 \times 10^{-3}$ mm^2/s, $p = 0.034$).

For patients with mixed pattern, the ADC_{mean} value was significantly increased from baseline to post-treatment ($0.81 \pm 0.12 \times 10^{-3}$ mm^2/s *vs.* $1.11 \pm 0.46 \times 10^{-3}$ mm^2/s, $p = 0.005$). Furthermore, the ADC_{mean} was significantly increased following treatment in deep responders ($0.83 \pm 0.12 \times 10^{-3}$ mm^2/s *vs.* $1.12 \pm 0.51 \times 10^{-3}$ mm^2/s, $p = 0.024$). However, the ADC_{mean} did not change significantly following treatment ($0.74 \pm 0.13 \times 10^{-3}$ mm^2/s *vs.* $1.09 \pm 0.29 \times 10^{-3}$ mm^2/s, $p = 0.089$) in the non-deep responder group.

The ANOVA test indicated that the baseline ADC_{mean} value of patients with focal pattern was significant higher compared with those with diffuse pattern ($p = 0.011$).

3.3. Per lesion analysis

In the per lesion analysis, 1173 lesions from these 72 patients were included. Fig. 2 presents the per lesion analysis for changes of ADC_{mean}.

The ADC_{mean} value of all lesions at baseline and post-treatment was $0.80 \pm 0.23 \times 10^{-3}$ mm^2/s and $0.86 \pm 0.69 \times 10^{-3}$ mm^2/s, respectively. Following treatment, there was a significant increase in ADC_{mean} value for all lesions ($p = 0.01$). There was a significant change of ADC_{mean} value in both the deep responder group ($0.82 \pm 0.23 \times 10^{-3}$ mm^2/s *vs.* $0.84 \pm 0.71 \times 10^{-3}$ mm^2/s, $p = 0.000$) and non-deep responder group ($0.73 \pm 0.19 \times 10^{-3}$ mm^2/s *vs.* $0.94 \pm 0.59 \times 10^{-3}$ mm^2/s, $p = 0.000$).

A total of 327 FLs (including FLs of patients with mixed pattern) were detected by WB-DWI MRI. The most frequently involved structures were the pelvis (98). Other involved sites included lumbar spine (67), ribs (48), thoracic spine (39), femur and lower leg (20), clavicle (15), shoulder girdle (15), humerus (12), cervical spine (8), and sternum (5).

For 327 FLs, the ADC_{mean} value was significantly increased from baseline to post-treatment ($0.93 \pm 0.26 \times 10^{-3}$ mm^2/s *vs.*

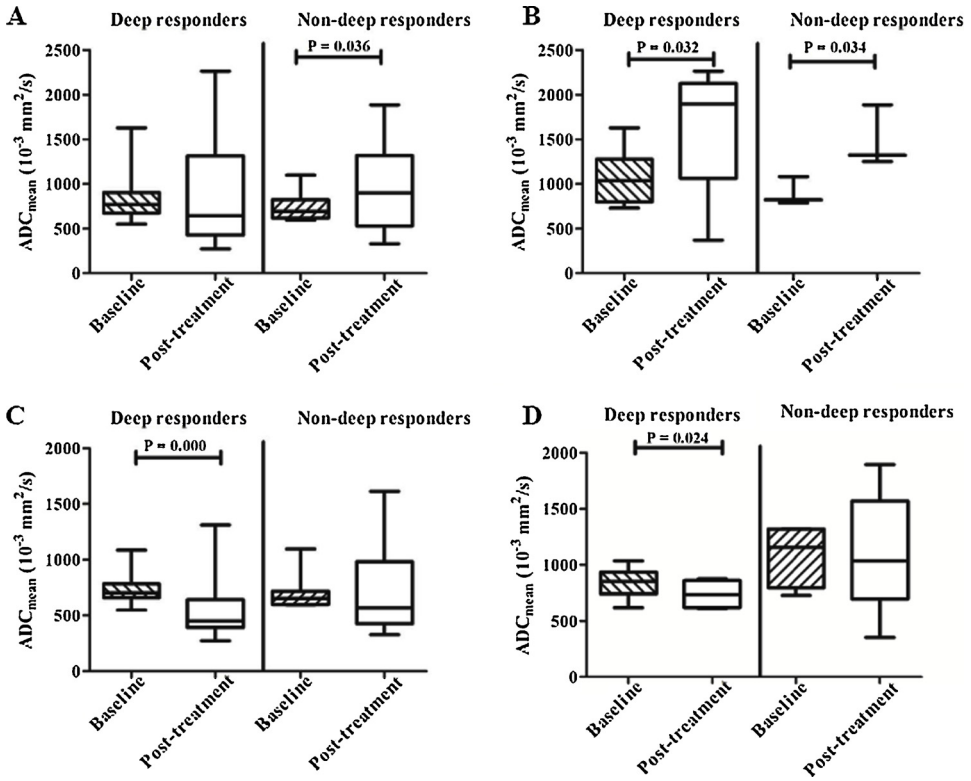

Fig. 1. Box and whisker plots of per patient-based ADC_{mean} changes in deep responders and non-deep responders regarding all (A), focal (B), diffuse (C) and mixed (D) patterns.

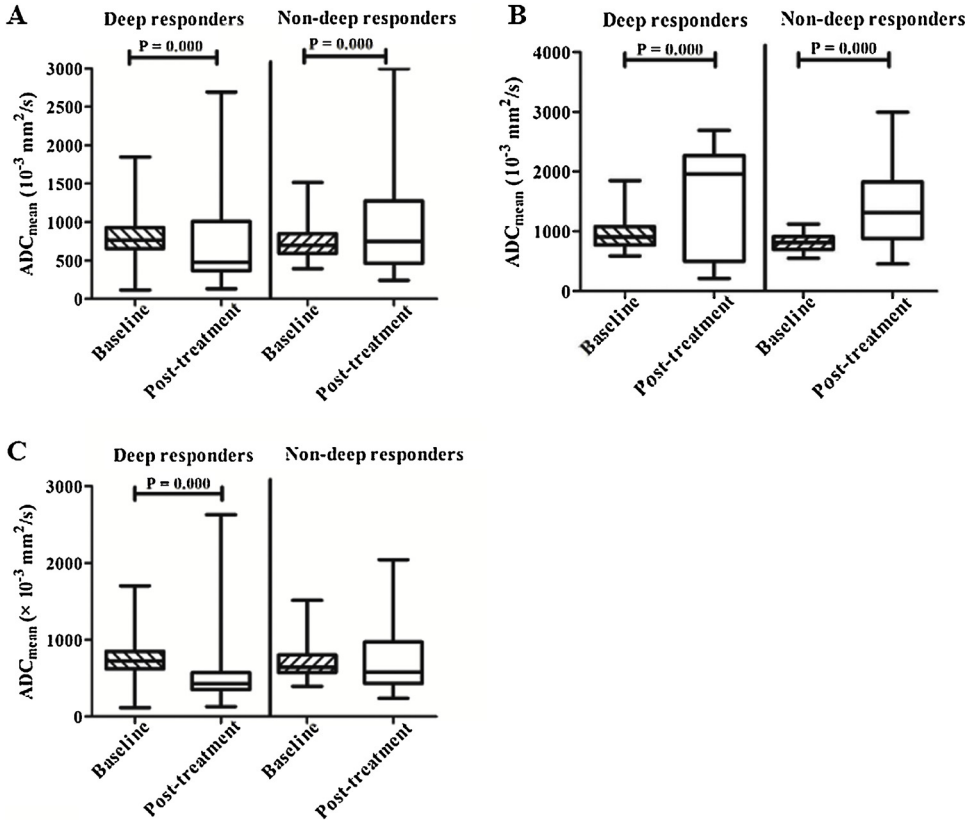

Fig. 2. Box and whisker plots of per lesion-based ADC_{mean} changes in deep responders and non-deep responders regarding all (A), focal (B) and diffuse (C) patterns.

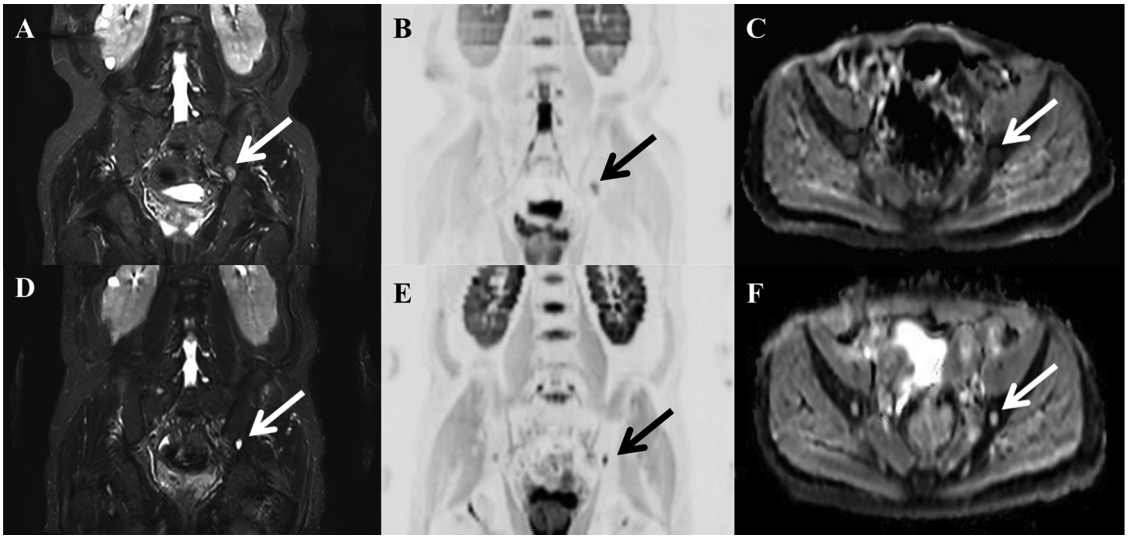

Fig. 3. Representative images of the WB MRI scan of a 60-year-old male patient prior to (A–C) and following four cycles (D–F) of induction PAD chemotherapy. A, D Coronal whole-body T2 TIRM; B, E Coronal b_{700} "PET-like" images; C, F Axial ADC map depicting an FL in left pelvis (arrows). Comparison between baseline and following four cycles of treatment revealed that there were a reduction in eTV and an increase in ADC_{mean} of the FL.

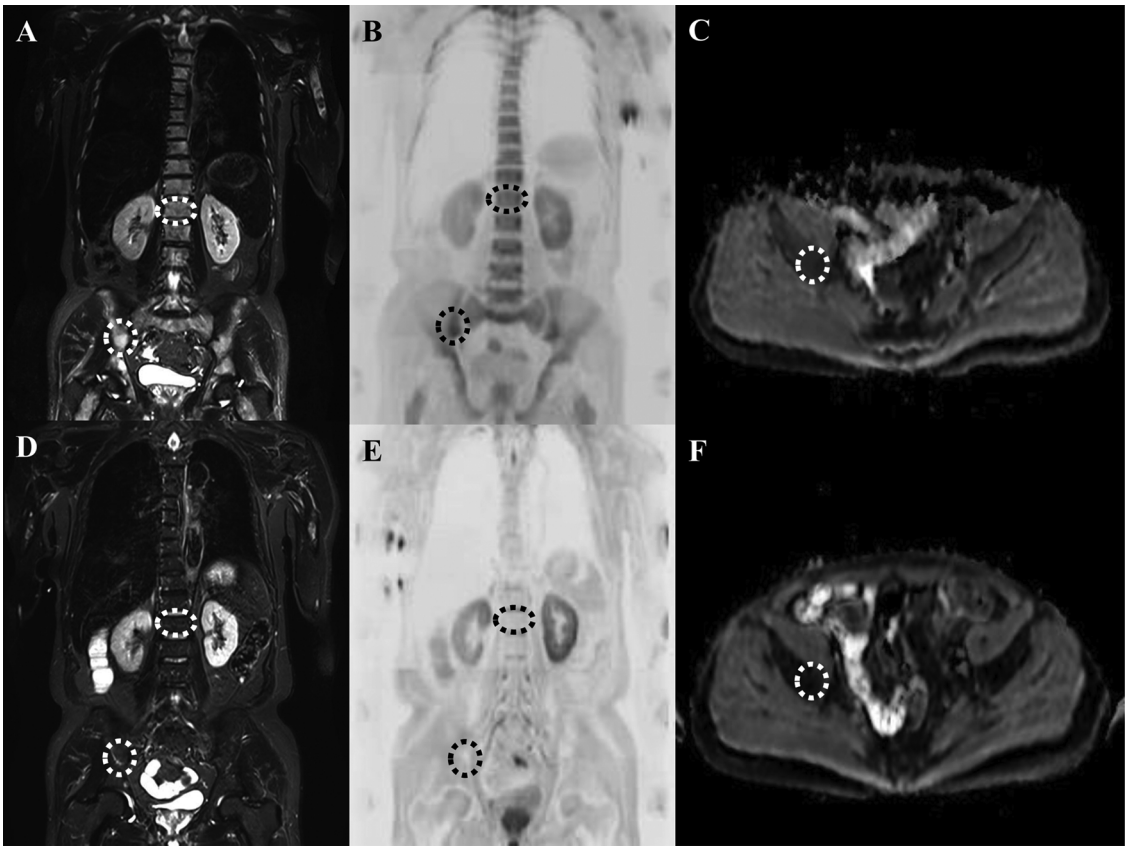

Fig. 4. Representative images of the WB MRI scan of a 55-year-old male patient prior to (A–C) and following five cycles (D–F) of induction PTD chemotherapy. A, D Coronal whole-body T2 TIRM; B, E Coronal b_{700} "PET-like" images; C, F Axial ADC map depicting diffuse pattern lesions in vertebral column, pelvis and femora (circles). Comparison between baseline and following five cycles of treatment revealed that there was a decrease in ADC_{mean} of the diffuse lesions.

$1.52 \pm 0.81 \times 10^{-3}$ mm^2/s, p = 0.000). Moreover, the ADC_{mean} was significantly increased following treatment in deep responders ($0.97 \pm 0.28 \times 10^{-3}$ mm^2/s *vs.* $1.55 \pm 0.85 \times 10^{-3}$ mm^2/s, p = 0.000) and non-deep responders ($0.81 \pm 0.14 \times 10^{-3}$ mm^2/s *vs.* $1.41 \pm 0.64 \times 10^{-3}$ mm^2/s, p = 0.000).

For 846 representative diffuse lesions (including representative diffuse lesions of patients with mixed pattern), the ADC_{mean} value was significantly decreased from baseline to post-treatment ($0.75 \pm 0.19 \times 10^{-3}$ mm^2/s *vs.* $0.60 \pm 0.41 \times 10^{-3}$ mm^2/s, p = 0.000). Moreover, the ADC_{mean} value significantly decreased following treatment in deep responders ($0.76 \pm 0.18 \times 10^{-3}$ mm^2/s *vs.* $0.55 \pm 0.38 \times 10^{-3}$ mm^2/s, p = 0.000). In the non-deep responder group, the ADC_{mean} value did not significantly change following treatment ($0.70 \pm 0.19 \times 10^{-3}$ mm^2/s *vs.* $0.77 \pm 0.49 \times 10^{-3}$ mm^2/s,

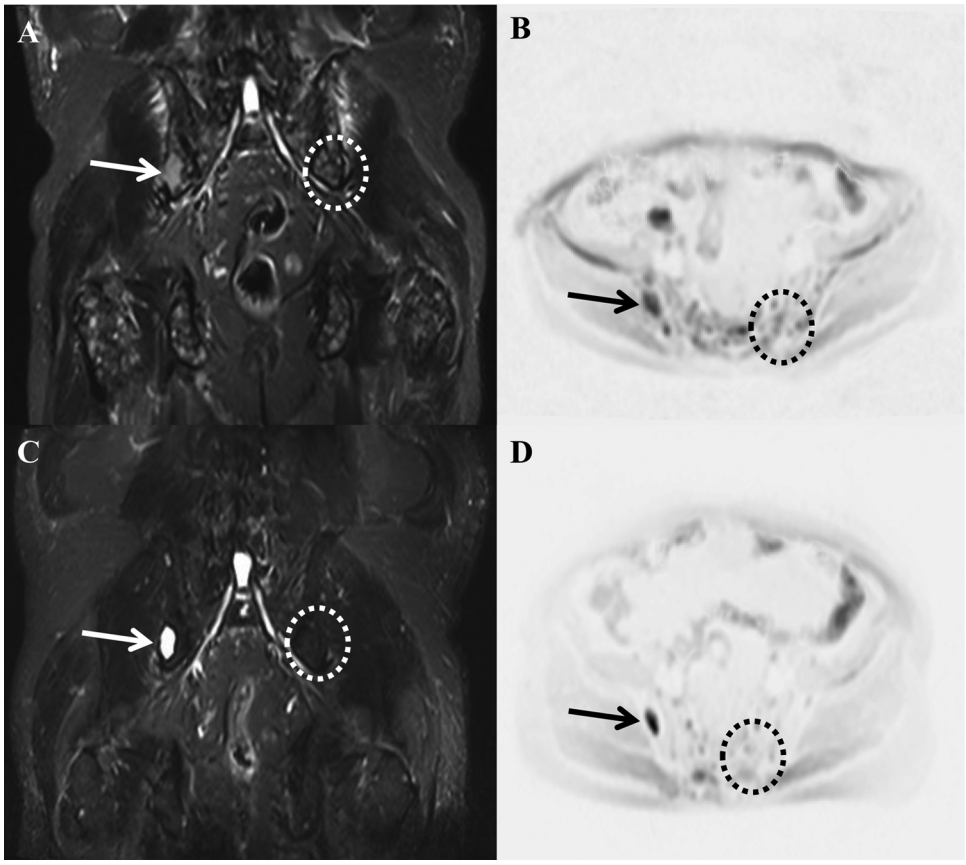

Fig. 5. Representative images of the WB MRI scan of a 67-year-old male patient prior to (A–B) and following four cycles (C–D) of induction PTD chemotherapy. A, C Coronal whole-body T2 TIRM; B, D Axial b_{700} "PET-like" images depicting an FL in right pelvis (arrows) and diffuse pattern lesions in pelvis and femora (circles). Comparison between baseline and following five cycles of treatment revealed that there were a reduction of eTV and an increase in ADC_{mean} of the FL, while a decrease in ADC_{mean} of the diffuse lesions was found.

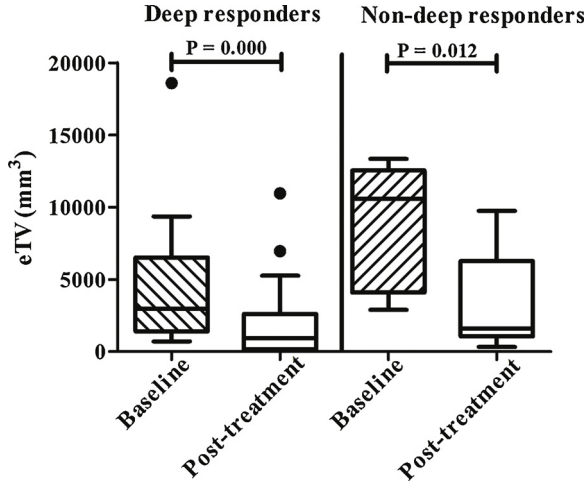

Fig. 6. Box and whisker plots of per lesion-based eTV changes in deep responders and non-deep responders regarding focal patterns.

p = 0.441). The baseline ADC_{mean} value of patients with focal pattern was significant higher than that of patients with diffuse pattern (p = 0.000).

Fig. 3–5 present examples of lesions at baseline and post-treatment in responding patients with different patterns.

3.4. eTV analysis

A total of 109 representative FLs in 31 patients (focal pattern and mixed pattern) were selected for per patient-based eTV analysis. The eTV was significantly decreased following treatment in all patients ($14.48 \pm 42.91 \times 10^3$ mm^3 *vs.* $4.29 \pm 11.69 \times 10^3$ mm^3, p = 0.000). Moreover, eTV was significantly changed in both the deep responder group ($16.24 \pm 48.82 \times 10^3$ mm^3 *vs.* $4.50 \pm 13.23 \times 10^3$ mm^3, p = 0.000) and non-deep responder group ($8.46 \pm 4.31 \times 10^3$ mm^3 *vs.* $3.55 \pm 3.45 \times 10^3$ mm^3, p = 0.012) (Fig. 6).

3.5. ROC curves

ROC analysis of percentage change in ADC_{mean} of diffuse lesions indicated that a 33.07% decrease in ADC_{mean} correctly identified deep response to treatment with a sensitivity of 64.5% and a specificity of 77% (AUC 0.75, 95% confidence interval 0.713 - 0.768, p = 0.000).

ROC analysis of baseline ADC_{mean} between increase and decrease of post-treatment ADC_{mean} revealed a significant AUC of 0.612 (95% confidence interval 0.577 - 0.647, p = 0.000), and its cutoff in baseline ADC_{mean} value was 0.808×10^{-3} mm^2/s, predicting increase of post-treatment ADC_{mean} with a sensitivity of 54.09% and a specificity of 68.05% (Fig. 7).

4. Discussion

In the present study, we investigated the feasibility of using WB-DWI MRI for evaluation of response in MM patients following bortezomib-based therapy and explored the direction of ADC changes upon treatment. We observed a different trend of ADC_{mean} change following bortezomib-based treatment in patients with different DWI MRI infiltration patterns. For patients with focal pattern, the ADC_{mean} value was significantly increased from baseline to post-treatment. However, the ADC_{mean} value was significantly decreased following treatment in patients with diffuse pattern. Diffuse lesions showed a significantly decreased ADC_{mean} value in deep responders, whereas no significant variation of ADC_{mean} value in FLs was found between deep responders and non-deep responders.

In recent years, some small cohort studies have investigated the

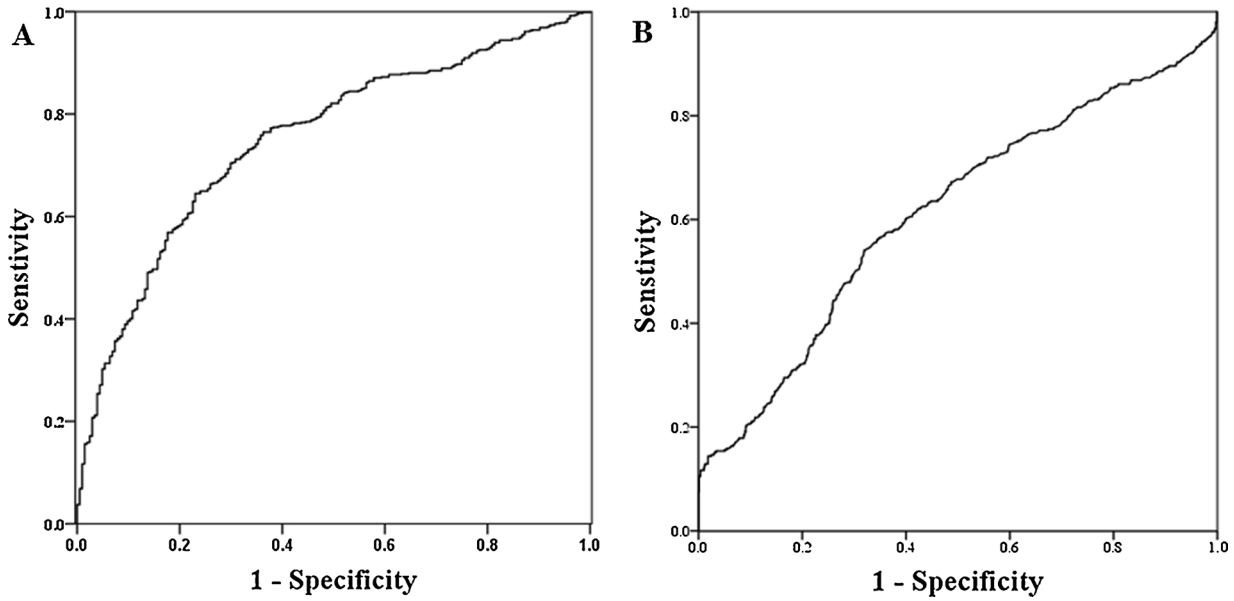

Fig. 7. ROC curves of percentage change in ADC_{mean} of diffuse lesions for prediction of deep response (A) and baseline ADC_{mean} for the prediction of ADC_{mean} change following treatment (B).

ADC change in MM patients following treatment. The majority of these studies have reported treatment-related increases in ADC [10–13,20–22]. However, limited by a small cohort size, only focal or diffuse lesions have been studied, or no information regarding the infiltration pattern has been provided. It is well known that normal fatty bone marrow has a low ADC value due to low water content and impeded water movement [23]. In MM patients, increased ADC values are found in focal or diffuse lesions, which are characterized by reduced number of adipocytes, increased water content, and increased proportion of plasma cells [24]. After effective anti-myeloma treatment, the marrow hemorrhage and edema because of tumor cell death and vascular congestion result in a further increase in ADC value [25]. Messiou et al. have observed an initial increase in ADC at 4–6 weeks, reflecting necrosis/edema followed by a decrease in ADC at 20 weeks caused by a return of normal marrow in responders [26]. In this study, we observed the opposite direction of ADC changes upon treatment between patients with diffuse pattern and those with focal pattern. This finding might be attributed to the fact that single FL is characterized by infiltration of more tumor cells and higher baseline ADC value compared with the diffuse lesion [27]. It may take longer time for FLs to recovery from tumor cells to normal marrow fat.

Latifoltojar et al. have observed a significant increase in ADC value of focal myeloma lesions in responders at 21 weeks from therapy compared with the non-responders [13]. However, Messiou et al. have reported that there is no significant difference of ADC value between responders and non-responders at 20 weeks [26]. In the present study, the ADC_{mean} was significantly increased following treatment in both deep responders and non-deep responders at 21 weeks, showing that it was still a challenge to evaluate deep response using ADC change in focal MM. On the one hand, in this era of novel regimens, the majority of patients, including some non-deep responders, are likely to benefit from the treatment [28]. On the other hand, there is a great overlap between the marrow edema/necrosis and high-grade bone marrow infiltration of myeloma cells, which exhibits high ADC values [10].

Few studies have investigated ADC values to evaluate the response in MM patients with diffuse pattern. In a study by Lacognata et al., 18 MM patients undergo WB-DWI MRI at baseline, and their status is evaluated prospectively at 21 weeks after bortezomib-based induction chemotherapy. In this report, there is no association between response and therapy considering ADC value in diffuse pattern lesions [20]. However, our present results were opposite to those of Lacognata et al., showing that WB-MRI DWI was useful in evaluating response to therapy in MM patients with diffuse pattern. In the study by Lacognata et al., the mean value of baseline ADC is $0.93 \pm 0.3 \times 10^{-3}\,mm^2/s$ for patients with diffuse lesions, indicating that more patients with moderate or severe pattern are included.

In line with previous reports, we observed that eTV was significantly decreased following treatment in all the patients [11,13]. Our analyses indicated that eTV had no value in distinguishing deep response in MM patients, which was also consistent with previous findings [13,21].

In our study, the ADC_{mean} was significantly increased after treatment in patients with higher baseline ADC_{mean} value. Baseline ADC_{mean} at a specific value ($0.808 \times 10^{-3}\ mm^2/s$) yielded a maximum specificity and sensitivity in predicting changes of post-treatment ADC_{mean}. However, such diagnostic accuracy (sensitivity and specificity < 70%) might not bring confidence for physicians.

To the best of our knowledge, this study was the largest single center cohort determining the feasibility of WB-DWI MRI for evaluation of response in MM patients following bortezomib-based therapy. However, there were still some limitations in the present study. The retrospective character represents the main limitation of this study. Further prospective studies are required to confirm these results. Furthermore, the only time point investigated in the present study is the end of the induction period. In the future, multiple-time-point analyses are needed to find the optimum time point for assessment of treatment response.

Collectively, the ADC_{mean} value was significantly decreased in MM patients with diffuse pattern, while it was significantly increased in those with focal pattern following bortezomib-based treatment. WB-DWI MRI could be used to discriminate deep response to induction treatment in MM patients with diffuse infiltration pattern. Moreover, the baseline ADC_{mean} might have a potential to predict the trend of ADC_{mean} change following treatment.

Funding

This study was supported by National Natural Science Foundation of China (No. 81601522), Natural Science Foundation of Jiangsu Province (No. BK20160348), Medical Youth Talent Project of Jiangsu Province (No. QNRC2016749) and Suzhou People's Livelihood Science and Technology Project (SYS2019038).

Declaration of Competing Interest

The authors declare no conflict of interest.

References

[1] B.G. Hansford, R. Silbermann, Advanced imaging of multiple myeloma bone disease, Front. Endocrinol. (Lausanne) 9 (2018) 436.

[2] E. Terpos, D. Christoulas, M. Gavriatopoulou, Biology and treatment of myeloma related bone disease, Metabolism 80 (2018) 80–90.

[3] S.Z. Usmani, A. Hoering, M. Cavo, J.S. Miguel, H. Goldschmidt, R. Hajek, I. Turesson, J.J. Lahuerta, M. Attal, B. Barlogie, J.H. Lee, S. Kumar, S. Lenhoff, G. Morgan, S.V. Rajkumar, B.G.M. Durie, P. Moreau, Clinical predictors of long-term survival in newly diagnosed transplant eligible multiple myeloma - an IMWG Research Project, Blood Cancer J. 8 (12) (2018) 123.

[4] E. Scalzulli, S. Grammatico, F. Vozella, M.T. Petrucci, Proteasome inhibitors for the treatment of multiple myeloma, Expert Opin. Pharmacother. 19 (4) (2018) 375–386.

[5] S. Kumar, B. Paiva, K.C. Anderson, B. Durie, O. Landgren, P. Moreau, N. Munshi, S. Lonial, J. Bladé, M.V. Mateos, M. Dimopoulos, E. Kastritis, M. Boccadoro, R. Orlowski, H. Goldschmidt, A. Spencer, J. Hou, W.J. Chng, S.Z. Usmani, E. Zamagni, K. Shimizu, S. Jagannath, H.E. Johnsen, E. Terpos, A. Reiman, R.A. Kyle, P. Sonneveld, P.G. Richardson, P. McCarthy, H. Ludwig, W. Chen, M. Cavo, J.L. Harousseau, S. Lentzsch, J. Hillengass, A. Palumbo, A. Orfao, S.V. Rajkumar, J.S. Miguel, H. Avet-Loiseau, International Myeloma Working Group consensus criteria for response and minimal residual disease assessment in multiple myeloma, Lancet Oncol. 17 (8) (2016) e328–e346.

[6] B.G. Durie, J.L. Harousseau, J.S. Miguel, J. Bladé, B. Barlogie, K. Anderson, M. Gertz, M. Dimopoulos, J. Westin, P. Sonneveld, H. Ludwig, G. Gahrton, M. Beksac, J. Crowley, A. Belch, M. Boccadaro, M. Cavo, I. Turesson, D. Joshua, D. Vesole, R. Kyle, R. Alexanian, G. Tricot, M. Attal, G. Merlini, R. Powles, P. Richardson, K. Shimizu, P. Tosi, G. Morgan, S.V. Rajkumar, International Myeloma Working Group. International uniform response criteria for multiple myeloma, Leukemia 20 (9) (2006) 1467–1473.

[7] G. Petralia, A.R. Padhani, P. Pricolo, F. Zugni, M. Martinetti, P.E. Summers, L. Grazioli, S. Colagrande, A. Giovagnoni, M. Bellomi, Italian Working Group on Magnetic Resonance. Whole-body magnetic resonance imaging (WB-MRI) in oncology: recommendations and key uses, Leuk. Lymphoma (2018) 1–11.

[8] A. Stecco, F. Buemi, A. Iannessi, A. Carriero, A. Gallamini, Current concepts in tumor imaging with whole-body MRI with diffusion imaging (WB-MRI-DWI) in multiple myeloma and lymphoma, Leuk. Lymphoma (2018) 1–11.

[9] M.A. Dimopoulos, J. Hillengass, S. Usmani, E. Zamagni, S. Lentzsch, F.E. Davies, N. Raje, O. Sezer, S. Zweegman, J. Shah, A. Badros, K. Shimizu, P. Moreau, C.S. Chim, J.J. Lahuerta, J. Hou, A. Jurczyszyn, H. Goldschmidt, P. Sonneveld, A. Palumbo, H. Ludwig, M. Cavo, B. Barlogie, K. Anderson, G.D. Roodman, S.V. Rajkumar, B.G. Durie, E. Terpos, Role of magnetic resonance imaging in the management of patients with multiple myeloma: a consensus statement, J. Clin. Oncol. 33 (6) (2015) 657–664.

[10] M. Horger, K. Weisel, W. Horger, A. Mroue, M. Fenchel, M. Lichy, Whole-body diffusion-weighted MRI with apparent diffusion coefficient mapping for early response monitoring in multiple myeloma: preliminary results, AJR Am. J. Roentgenol. 196 (6) (2011) W790–5.

[11] A. Latifoltojar, M. Hall-Craggs, N. Rabin, R. Popat, A. Bainbridge, N. Dikaios, M. Sokolska, A. Rismani, S. D'Sa, S. Punwani, K. Yong, Whole body magnetic resonance imaging in newly diagnosed multiple myeloma: early changes in lesional signal fat fraction predict disease response, Br. J. Haematol. 176 (2) (2017) 222–233.

[12] S.L. Giles, C. Messiou, D.J. Collins, V.A. Morgan, C.J. Simpkin, S. West, F.E. Davies, G.J. Morgan, N.M. deSouza, Whole-body diffusion-weighted MR imaging for assessment of treatment response in myeloma, Radiology 271 (3) (2014) 785–794.

[13] A. Latifoltojar, M. Hall-Craggs, A. Bainbridge, N. Rabin, R. Popat, A. Rismani, S. D'Sa, N. Dikaios, M. Sokolska, M. Antonelli, S. Ourselin, K. Yong, S.A. Taylor, S. Halligan, S. Punwani, Whole-body MRI quantitative biomarkers are associated significantly with treatment response in patients with newly diagnosed symptomatic multiple myeloma following bortezomib induction, Eur. Radiol. 27 (12) (2017) 5325–5336.

[14] J.C. Dutoit, E. Claus, F. Offner, L. Noens, J. Delanghe, K.L. Verstraete, Combined evaluation of conventional MRI, dynamic contrast-enhanced MRI and diffusion weighted imaging for response evaluation of patients with multiple myeloma, Eur. J. Radiol. 85 (2) (2016) 373–382.

[15] M. Horger, J. Fritz, W.M. Thaiss, H. Ditt, K. Weisel, M. Haap, C. Kloth, Comparison of qualitative and quantitative CT and MRI parameters for monitoring of longitudinal spine involvement in patients with multiple myeloma, Skeletal Radiol. 47 (3) (2018) 351–361.

[16] J. Hillengass, T. Bäuerle, R. Bartl, M. Andrulis, F. McClanahan, F.B. Laun, C.M. Zechmann, R. Shah, B. Wagner-Gund, D. Simon, C. Heiss, K. Neben, A.D. Ho, H.P. Schlemmer, H. Goldschmidt, S. Delorme, B. Stieltjes, Diffusion-weighted imaging for non-invasive and quantitative monitoring of bone marrow infiltration in patients with monoclonal plasma cell disease: a comparative study with histology, Br. J. Haematol. 153 (6) (2011) 721–728.

[17] C. Messiou, J. Hillengass, S. Delorme, F.E. Lecouvet, L.A. Moulopoulos, D.J. Collins, M.D. Blackledge, N. Abildgaard, B. Østergaard, H.P. Schlemmer, O. Landgren, J.T. Asmussen, M.F. Kaiser, A. Padhani, Guidelines for acquisition, interpretation, and reporting of whole-body MRI in myeloma: myeloma response assessment and diagnosis system (MY-RADS), Radiology 291 (1) (2019) 5–13.

[18] A. Stäbler, A. Baur, R. Bartl, R. Munker, R. Lamerz, M.F. Reiser, Contrast enhancement and quantitative signal analysis in MR imaging of multiple myeloma: assessment of focal and diffuse growth patterns in marrow correlated with biopsies and survival rates, AJR Am. J. Roentgenol. 167 (4) (1996) 1029–1036.

[19] B.G. Durie, The role of anatomic and functional staging in myeloma: description of Durie/Salmon plus staging system, Eur. J. Cancer 42 (2006) 1539–1543.

[20] C. Lacognata, F. Crimì, A. Guolo, C. Varin, E. De March, S. Vio, A. Ponzoni, G. Barilà, A. Lico, A. Branca, E. De Biasi, F. Gherlinzoni, V. Scapin, E. Bissoli, T. Berno, R. Zambello, Diffusion-weighted whole-body MRI for evaluation of early response in multiple myeloma, Clin. Radiol. 72 (10) (2017) 850–857.

[21] C. Wu, J. Huang, W.B. Xu, Y.J. Guan, H.W. Ling, J.Q. Mi, H. Yan, Discriminating depth of response to therapy in multiple myeloma using whole-body diffusion-weighted MRI with apparent diffusion coefficient: preliminary results from a single-center study, Acad. Radiol. 25 (7) (2018) 904–914.

[22] P.A. Bonaffini, D. Ippolito, A. Casiraghi, V. Besostri, C.T. Franzesi, S. Sironi, Apparent diffusion coefficient maps integrated in whole-body MRI examination for the evaluation of tumor response to chemotherapy in patients with multiple myeloma, Acad. Radiol. 22 (9) (2015) 1163–1171.

[23] A. Stecco, F. Buemi, A. Iannessi, A. Carriero, A. Gallamini, Current concepts in tumor imaging with whole-body MRI with diffusion imaging (WB-MRI-DWI) in multiple myeloma and lymphoma, Leuk. Lymphoma 12 (2018) 1–11.

[24] J.C. Dutoit, K.L. Verstraete, MRI in multiple myeloma: a pictorial review of diagnostic and post-treatment findings, Insights Imaging 7 (4) (2016) 553–569.

[25] A.R. Padhani, D.M. Koh, D.J. Collins, Whole-body diffusion-weighted MR imaging in cancer: current status and research directions, Radiology 261 (3) (2011) 700–718.

[26] C. Messiou, S. Giles, D.J. Collins, S. West, F.E. Davies, G.J. Morgan, N.M. Desouza, Assessing response of myeloma bone disease with diffusion-weighted MRI, Br. J. Radiol. 85 (1020) (2012) e1198–203.

[27] V. Koutoulidis, S. Fontara, E. Terpos, F. Zagouri, D. Matsaridis, D. Christoulas, E. Panourgias, E. Kastritis, M.A. Dimopoulos, L.A. Moulopoulos, Quantitative diffusion-weighted imaging of the bone marrow: an adjunct tool for the diagnosis of a diffuse MR imaging pattern in patients with multiple myeloma, Radiology 282 (2) (2017) 484–493.

[28] S. Lonial, K.C. Anderson, Association of response endpoints with survival outcomes in multiple myeloma, Leukemia 28 (2) (2014) 258–268.